J Mater Sci (2010) 45:1487–1494
DOI 10.1007/s10853-009-4109-0

Novel structural properties of the lead–vanadate–tellurate glass ceramics

**M. Rada · E. Culea · S. Rada · V. Maties ·
P. Pascuta**

Received: 19 July 2009 / Accepted: 3 December 2009 / Published online: 23 December 2009

Abstract In this paper, we have examined and analyzed the effects of systematic intercalation of the lead ions on vanadate–tellurate glass ceramics with interesting results. The structural properties of the lead–vanadate–tellurate glass ceramics of compositions $x\mathrm{PbO}\cdot(100-x)[6\mathrm{TeO}_2\cdot 4\mathrm{V}_2\mathrm{O}_5]$, $x = 0 - 100$ mol%, are reported for the first time. It has been shown by X-ray diffraction that single-phase homogeneous glasses with a random network structure can be obtained in this system. Among these unconventional lead–vanadate–tellurate glass ceramics, we found that network formers are good host material for lead ions and are capable to intercalate a variety of species such as $\mathrm{Te}_2\mathrm{V}_2^{5+}\mathrm{O}_9$, $\mathrm{Pb}_3(\mathrm{V}^{5+}\mathrm{O}_4)_2$, $\mathrm{Pb}_2\mathrm{V}_2^{5+}\mathrm{O}_7$, and $\mathrm{V}_2\mathrm{O}_5$-rich amorphous phase. On the other hand, these glass ceramics contain V^{4+} and V^{5+} ions necessary for the electrical conduction. Based on these experimental results, we propose that the $\mathrm{V}^{4+}{=}\mathrm{O}$ bonds are created by two different mechanisms: the first of reduction of V^{5+} ions to V^{4+} ions and thus of creation of $\mathrm{V}^{4+}{=}\mathrm{O}$ bonds.

Introduction

Tellurate glasses possess interesting glass-forming ability, glass structure, no hydroscopic properties, and low melting point. Tellurate glasses containing a large amount of transition metal oxides, such as $\mathrm{V}_2\mathrm{O}_5$, have relatively higher conductivity [1].

Among vanadate glasses, lead vanadate has received greater attention as a new branch in semiconducting glasses because of its wider glass-forming region in the phase diagram, and its possible technological applications in threshold switching, memory switching, electrical threshold, electrochemical batteries, and optical switching devices [2–4].

Structures of tellurate glasses, which have high thermal expansion coefficients and low glass transition temperature, are known to be different from silicate glasses [5]. Change in glass composition affect the induced optical absorption due to several reasons, namely, the polarization power of network formers, modifiers, their coordination numbers, the concentration of non-bridging oxygen, the presence of multivalent network forming, and modifying ions.

Previous studies on vanadium tellurate glasses showed that their mechanical properties depend on the percentage of $\mathrm{V}_2\mathrm{O}_5$ [6]. When the $\mathrm{V}_2\mathrm{O}_5$ concentration is below 20 mol%, the three-dimensional tellurate networks are partially broken by formation of $[\mathrm{TeO}_3]$ trigonal pyramids which in turn reduce the glass rigidity [7–12]. When the $\mathrm{V}_2\mathrm{O}_5$ concentration is above 20 mol%, the glass structure changed from continuous tellurate network to the continuous vanadate network [7–9].

In brief, despite many characterizations, the structure of TeO_2–$\mathrm{V}_2\mathrm{O}_5$ glasses is still subject to discussion. The purpose of this paper was to approach the structure of vanadate–tellurate glasses when the $\mathrm{V}_2\mathrm{O}_5$ concentration is 40 mol% using the infrared spectroscopy and X-ray diffraction.

For many years, glasses containing transition metal ions have attracted attention because of their potential applications in electrochemical, electronic, and electro-optic devices [13].

Oxide glasses doped with the transition metal oxides such as $\mathrm{V}_2\mathrm{O}_5$ are known to exhibit semiconducting properties [14–17]. The investigation of the glasses containing

---

M. Rada · E. Culea · S. Rada (✉) · V. Maties · P. Pascuta
Department of Physics, Technical University of Cluj-Napoca,
400020 Cluj-Napoca, Romania
e-mail: simona.rada@phys.utcluj.ro; radasimona@yahoo.com

divalent ions such as Pb^{2+} is particularly important due important role of the lead ions both in formation and modification of glass structure [18–20].

Naturally, a glass based on a mixture of both transition and alkali metals exhibits a mixed ionic and electronic conductivity. In the last few years, the study of such mixed electronic–ionic conductors grew rapidly due to the numerous potential applications of these materials as cathodes for electrochemical cells or smart windows for example. The conduction mechanism of these glasses was interpreted using the small polaron hoping model [21–23]. With alkaline or silver cations, tellurate based glasses are known to present a high ionic conductivity [24–27].

Understanding the dependence of physical properties on glass microstructure is critical for the design of materials suitable for specific applications. It seems then necessary to study the relationship between thermal treatments, crystalline phase formation, and structural properties of lead–vanadate–tellurate glasses. In this work, we attempt to study the relationship between these parameters.

Experimental

Lead–vanadate–tellurate glasses were prepared by mixing and melting of the appropriate amounts of tellurium dioxide, vanadium pentaoxide, and lead oxide (II) of high purity. Reagents were melted at 850 °C for 10 min and quenched. The glassy sample was subject to heat treatment applied at 275 °C for 8 h.

The samples were analyzed by means of X-ray diffraction using a XRD-6000 Shimadzu Diffractometer, with a monochromator of graphite for CuK_{α} radiation ($\lambda = 1.54$ Å) at room temperature.

The structure of the glasses was investigated by infrared transmission spectra in KBr matrices were recorded in the range from 400 to 1200 cm^{-1} using a JASCO FTIR 6200 spectrometer.

Results and discussion

In order to valorization of lead–vanadate–tellurate glasses, the devitrification behavior of these samples is reported. The controlled crystallization of this system is commonly employed to produce glass ceramics with desirable properties.

The X-ray diffraction patterns reveal any crystalline phase in the heat-treated samples at 275 °C for 8 h. By increasing the lead oxide content up to 100 mol%, X-ray diffraction analysis shows following:

(i) The composition of the glass ceramics with the PbO concentration up to 40 mol% was found to consist mainly of the $Te_2V_2O_9$ crystalline phase and little V_2O_5-rich amorphous phase (Fig. 1).

(ii) Surprising for samples with 50 and 60 mol% PbO can be observed two halos, characteristic of the amorphous compounds and the apparition a V_2O_5-rich amorphous phase [28–38] (Fig. 2).

V_2O_5 can be regarded as a layered structure in which [VO_5] square pyramids are connected by sharing corners and edges and thereby forming layers. This layer structure is composed of single corrugation slab with a corrugation step of 2.8 Å. The interactions between these layers are rather weak, as indicated by the exceptionally long V–O distance of ~2.8 Å. This structural peculiarity permits the

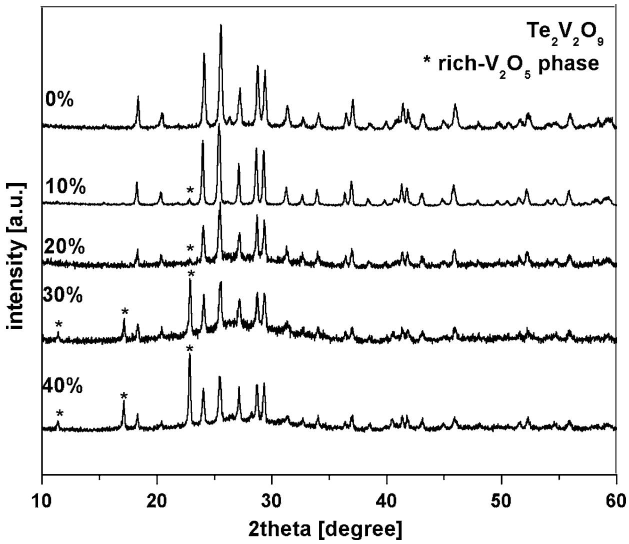

Fig. 1 X-ray diffraction patterns for heat-treated xPbO·(100 − x)[$6TeO_2 \cdot 4V_2O_5$] samples with x = 0–50% PbO

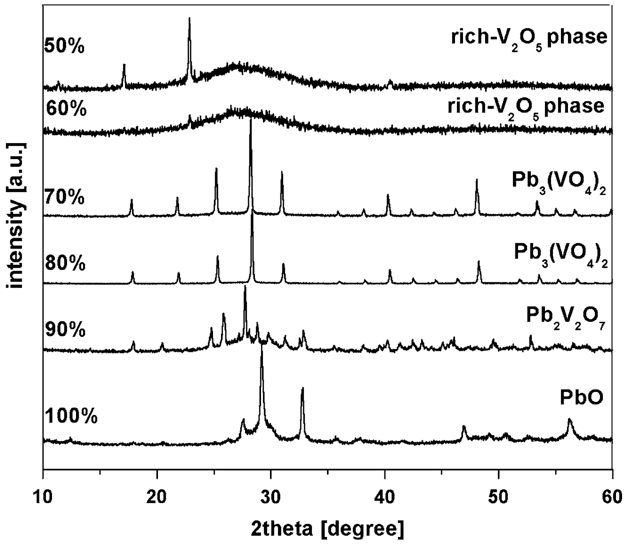

Fig. 2 X-ray diffraction patterns for heat-treated xPbO·(100 − x)[$6TeO_2 \cdot 4V_2O_5$] samples with x = 50–100% PbO

synthesis of phases intercalated vanadium oxide bronzes $M_xV_2O_5$ with cations embedded between the layers.

On the other hand, the V_2O_5-rich glasses in which V_2O_5 acts as the network former have the network structure mainly consisting of corner-sharing branched $[VO_4]$ tetrahedra of the same structural units as found in phosphate glasses. The network structure was reported to be made up of unaffected $[VO_5]$ units as in vitreous V_2O_5 and affected $[VO_5]$ units with alkaline earth ions in contrast to the vanadate glasses formed by conventional network formers in which only unaffected $[VO_5]$ units are present [33–42]. These glasses are known to contain V^{4+} and V^{5+} ions where the electrical conduction was attributed to the hopping of $3d^1$ unpaired electron from V^{4+} to V^{5+} site which induces a polarization of the vanadium ion around it and forms a polaron [27].

(iii) By increasing of the PbO content between 70 and 80 mol%PbO, X-ray pattern shows γ-$Pb_3(VO_4)_2$ crystalline phase. This substance has a rhombohedra lattice with $a = 5.76$ Å, $c = 20.368$ Å built of $[VO_4]$ tetrahedrons.

During the last few years some new antiferroelectrics of the displacement type were discovered. Particularly, the antiferroelectric phase transformation was found in lead orthovanadate, $Pb_3(VO_4)_2$ [43]. Lead orthovanadate exhibits two phase transitions in the vicinity of 0 °C (α phase) and 100 °C (β phase), respectively. The γ-phase has the rhombohedric structure when the temperature is higher than >100 °C. It is essentially a layer structure built on parallel $[VO_4]$ tetrahedrons.

The dielectric constant of $Pb_3(VO_4)_2$ has a maximum near 100 °C. A twinning structure observed below 100 °C in a polarized light beam along a three fold axis. These twins disappear above 100 °C. In transformation point of the sample shows sharp volume changes. These phenomena plus the absence of the dielectric hysteresis lops allowed the authors to propose the antiferroelectric properties of the lead orthovanadate [43].

(iv) In the structure of glass ceramic sample with 90 mol%PbO was found the $Pb_2V_2^{5+}O_7$ crystalline phase, while for the sample with 100 mol%PbO can be observed the PbO crystalline phase.

Crystalline PbO has two polymorphic forms: α-PbO (red color) has tetragonal phase, stable at low temperature and β-PbO (yellow color) has orthorhombic phase, stable at high temperature [43]. The α-PbO → β-PbO phase transition occurs at about 490 °C. At room temperature can be stable the β-PbO polymorphic form.

Both forms of PbO are layered structures consisting of $[PbO_4]$ pyramids arranged in planes perpendicular to the [0 0 1] direction. The oxygen atoms found that a sandwich between the lead atoms, each of which is at the apex of a $[PbO_4]$ pyramid. The difference is that the $[PbO_4]$ pyramidal units in β-PbO are destroyed, giving two sets of Pb–O distances [43–50]. The structure is built of layers having four bonds two of them have lengths 2.20 Å and the other two have lengths 2.49 Å. The shorter bonds delineate zigzag chains which are bonded into layers by the longer Pb–O bonds.

On the basis of IR-spectral investigations by comparing with known crystalline structure of V_2O_5, PbV_2O_6, and $Pb_2V_2O_7$, it is shown that the structural units in vanadate glasses are unaffected $[VO_5]$ units (a band at 1020 cm^{-1}), affected $[VO_5]$ units (bands at 950–970 cm^{-1}), V_2O_7 pyrovanadate units (bands at 780 and 860 cm^{-1}), and $[VO_4]$ isolated tetrahedral (a band at 760 cm^{-1}) [37–43].

The IR spectrum of vitreous V_2O_5 is similar to that of the crystal. This fact means that the isolated V=O bonds from $[VO_5]$ trigonal bipyramids are preserved in the vitreous structure. The spectrum of crystalline V_2O_5 exhibited an intense band at 1020 cm^{-1} which is identified due to the vibrations of isolated V=O bonds in V_2O_5 polyhedra. This V=O bond will participate in the formation of layer structures. The spectrum also exhibits another intense absorption band centered at 820 cm^{-1}. This band is related to V–O–V chains and weak shoulder located at about 600 cm^{-1} corresponds to bending vibrations of vanadium ions [34].

The examination of the FTIR spectra of the xPbO·$(100 - x)[6TeO_2{\cdot}4V_2O_5]$ glass ceramics with $x = 0$–40 mol% (Figs. 3, 4) shows that the increase of PbO content strongly modifies the characteristic IR bands as follows:

(i) The bands at around 440–467 and 500–530 cm^{-1} are attributed to the vibrations of angular deformation of the V–O bond. According to the expected as these bands may be overlapped with that attributed to the bending mode of the

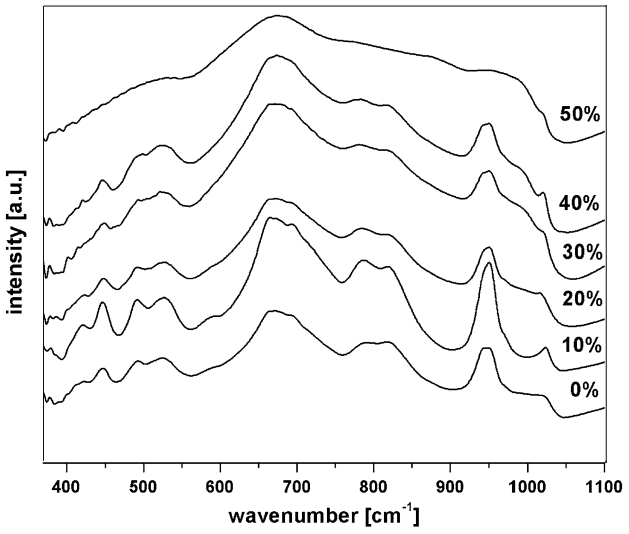

Fig. 3 FTIR spectra of xPbO·$(100 - x)[6TeO_2{\cdot}4V_2O_5]$ glass ceramics with $x = 0$–50% PbO

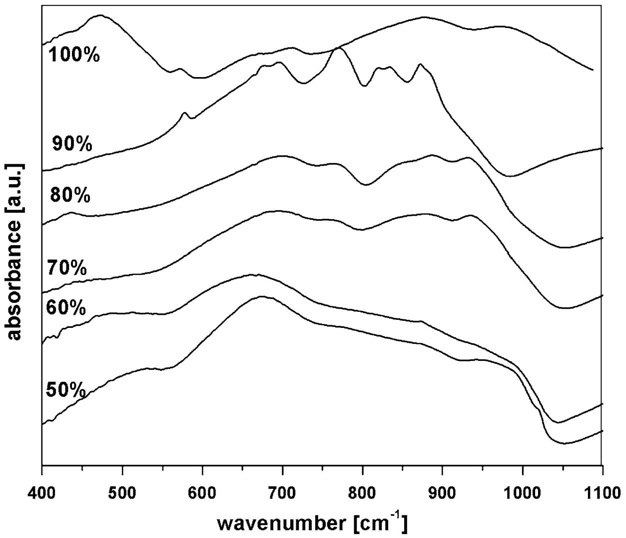

Fig. 4 FTIR spectra of xPbO·(100 − x)[6TeO$_2$·4V$_2$O$_5$] glass ceramics with $x = 50$–100% PbO

Te–O–Te or O–Te–O linkages. A new shoulder located at about 580 cm^{-1} appears in the spectrum of the glass ceramic with 10 and 90 mol% PbO. These shoulders can be associated with the bending vibrations of the vanadium ions.

(ii) The broader band centered at around 628–665 cm^{-1} are assigned to combination vibrations of (VO$_3$)$_n$ single chain or due to antisymmetric vibration modes of the V–O–V bonds. The larger band centered at ~680 cm^{-1} is assigned to the stretching mode of the [TeO$_4$] trigonal bypiramidal units with bridging oxygens [35].

The band located at about 780 cm^{-1} indicates the presence of the [TeO$_3$] structural units. The intensity of this band increases for sample with $x = 10$ mol% whereupon it decreases gradual at $x = 60$ mol% and after that it increases again attaining its maximum values at $x = 90$ mol%PbO.

The addition of 10 mol%PbO gives rise to the non-bridging oxygens because some [TeO$_4$] structural units were transformed in [TeO$_3$] structural units. The lead ions yield the deformation of the Te–O–Te linkages. The Pb^{2+} ions have also an affinity pronounced towards non-bridging-oxygens which acquires a negative charge reducing the positive charge on the lead ions.

(iii) The high-frequency band at 950 cm^{-1} is attributable not only to the [VO$_5$] structural units, but also to the branched [VO$_4$] units having one V=O bond. The observed band at 1020 cm^{-1} indicates the [VO$_5$] units with unaffected V=O bonds. Increasing proportions of PbO decrease the number of unaffected polyhedra and the higher frequency band located at about 950 cm^{-1} corresponds to the [VO$_5$] structural units and the affected polyhedrons.

By addition of 10 mol% PbO in the glass ceramic network, the intensity of band located at about 950 cm^{-1} becomes more intense. Then, the increase of PbO content up to 60 mol% produces a broader band located at about 970 cm^{-1}. The shifts of the band towards higher wavenumber suggest the existence of the [VO$_5$] → [VO$_4$] conversion process. Pursuant to, the presence of tetrahedral structural units of tellurium and vanadium facilitates the formation of homogeneous glass system for $x = 60$ mol%, in agreement with X-ray diffraction results.

For the composition corresponding to $x = 70$ and 80 mol% PbO, this band found again at 950 cm^{-1}. Then for $x = 90$ mol% the position of the band found towards lower wavenumber, namely ~860 cm^{-1} which corresponds to the pyrovanadate structural units.

For sample with $x = 70$ and 80 mol% PbO, the characteristic IR bands of the Pb$_3$(VO$_4$)$_2$ lead orthovanadate glass ceramics are observed at 760 and 870 cm^{-1} [36, 37]. The spectrum of Pb$_2$V$_2$O$_7$ pyrovanadate glass ceramics (sample with $x = 90$ mol%PbO) shows three maxima defined at 700, 780, and 860 cm^{-1} [29]. A new band centered at about 820 cm^{-1} can be assigned to the stretching vibrations of the V–O–V bridges from pyrovanadate [35].

(iv) A shoulder located at about 1020 cm^{-1} was observed in samples with $0 \le x \le 50$ mol% PbO. This is assigned to the V=O stretching mode. For samples with $10 \le x \le 60$ mol% PbO, the presence of the band centered at about 1020 cm^{-1} assigned to V=O bond indicates that the added PbO probably has a greater preference for tellurate network. A larger amount of the added PbO is used for the conversion of the tellurium atoms and hence the effect of Pb^{2+} ions on the V=O bond is very small. Surprising for samples with 50 and 60 mol% PbO can be observed two halos characteristic of the amorphous compounds and V$_2$O$_5$-rich amorphous phase, in agreement with X-ray diffraction pattern.

Another distinguished feature of samples with $60 \le x \le 90$ mol% is the shift of the band from 1020 cm^{-1} corresponding to the V^{5+} ions in octahedral coordination. With the addition of PbO, the shift of this vibration band towards lower wave number suggests the increase in bond length of isolated V=O bond. It is due to the fact that added PbO goes into the structure at the interstitial positions leaving its oxygens. Pb^{2+} ions now directly interact with the oxygen of the V=O bond, which are thereby weakened and the frequency of vibration shifts towards the lower wave number.

At higher amounts of PbO ($x > 50$ mol%), the gradual disappearance of the peak located at about 1020 cm^{-1} and the emergence of bands situated at about 995 cm^{-1} ($x = 30$ mol%), 982 cm^{-1} ($x = 50$ mol%), 935 cm^{-1} ($x =$ 70–80 mol%) clearly indicate the elongation of the V=O bond by different degrees, depending upon the position of Pb^{2+} ion with respect to V=O bond in the structure and the formation of non-bridging oxygens.

The added PbO also gives rise to the formation of non-bridging oxygens, thereby creating VO_4^{3-} units. It is obvious that the oxygen, which becomes non-bridging and acquires a negative charge, will move closer to the connected vanadium, consequently reducing the positive charge on the vanadium and thereby resulting in a decrease in the binding of other oxygens attached to this particular ion; the length of the V=O bond therefore increases. Also, due to the irregular and random distribution of atoms in the glass structure, the lead ions take positions interstitially that are more symmetrical among other units.

In order to see the quantitative estimation of the distribution of the various species represented by FTIR spectra, we will calculate the distribution by structural units based on the acid–base concept. Moreover, presence of multiple oxides in the glass always increases the tendency of network formers to attract oxygen ions due to competition between the cations themselves. This preference is decided by the electronegativity of the structural groups [47]. The unit which has higher electronegativity value picks up oxygen ion and gets modifier. This tendency increases further if the size of cations increases. A possible mechanism which explains the scheme of the structural modifications is represented on the basis of following equations:

(i) The species present in the sample with $x = 0$ are $Te_2V_2O_9$ crystalline phase, and structural units provided to the V_2O_5 and TeO_2. Variations observed in the FTIR spectra and X-ray diffraction patterns for sample with $x = 0$ are consistent with the scheme of modification explained above.

The following species should exist in this region:

$$Te_2V_2O_9 \equiv 2TeO_2{\cdot}V_2O_5$$
$$4TeO_2 \rightarrow 4\left[TeO_{2/2}O\right]^0$$
$$3V_2O_5 \rightarrow 2\left[VOO_{3/2}\right]^0 + 2\left[VO_{4/2}O\right]^{-1} + 2\left[VOO_{2/2}\right]^+$$

The modifier roles of the PbO can be represented as

$$PbO \rightarrow Pb^{2+} + O^{2-}$$

(ii) $x = 10$ mol%PbO

The lead ions are first inserted in the divalent state and they can be considered as modifiers because they have a strong affinity towards these groups containing non-bridging oxygens, which are negative-charged. Presence of multiple cations, tellurium, and vanadium in the glass ceramic to attract oxygen ions yield a competition between these cations. This preference is decided by the electronegativity of the structural groups. The $[TeOO_{3/2}]^-$ structural units (2.30) are readily available for charge compensation than the $[VOO_{4/2}]^-$ structural units because has higher electronegativity than the $[VOO_{4/2}]^{-1}$ structural units (2.20).

$$2\left[TeO_{2/2}O\right]^0 + O^{2-} \rightarrow 2\left[TeO_{3/2}O\right]^{-1}$$
$$Pb^{2+} + 2\left[TeO_{3/2}O\right]^{-1} \rightarrow 2\left[TeO_{2/2}O\right]^0 + PbO$$
$$PbO + 2\left[VOO_{3/2}\right]^0 \rightarrow Pb^{2+} + 2\left[VOO_{4/2}\right]^-$$
$$2\left[VO_{4/2}O\right]^{-1} + 2\left[VOO_{2/2}\right]^+ \rightarrow V_4O_{10} \quad (V_4O_{10} \equiv 2V_2O_5)$$

The two peaks at 1024 and 820 cm^{-1} suggest the presence of both terminal (V=O) and bridge (V–O–V) units in the trapped species [37]. These bands are close in frequency to two of the most prominent IR absorptions (1022 and 840 cm^{-1}) in solid vanadium pentaoxide which contains both bridging and terminal oxygens. A new shoulder appears at about 586 cm^{-1} indicating the bending modes of the V–O–V linkages.

Variations observed in the FTIR spectra for sample with $x = 10$ mol% are consistent with the scheme of modification explained above. The XRD pattern shows the existence of the $Te_2V_2O_7$ crystalline phase and V_2O_5-rich amorphous matrix.

(iii) $x = 20$–40 mol%PbO

$$2\left[TeO_{2/2}O\right]^0 + O^{2-} \rightarrow 2\left[TeO_{3/2}O\right]^{-1}$$
$$Pb^{2+} + 2\left[TeO_{3/2}O\right]^{-1} \rightarrow 2\left[TeO_{2/2}O\right]^0 + PbO$$
$$PbO + 2\left[TeO_{2/2}O\right]^0 \rightarrow Pb^{2+} + 2\left[TeO_{3/2}O\right]^{-1}$$
$$Pb^{2+} + 2\left[VOO_{4/2}\right]^{-1} \rightarrow PbO + 2\left[VO_{3/2}O\right]^0$$

This process of reconversion of the $[TeO_4]$ to $[TeO_3]$ structural units is evident from the removal of the vibrational bands of the $[TeO_4]$ structural units towards higher wavenumber and of the $[TeO_3]$ structural units towards lower wavenumber.

(iv) $x = 50$ mol%PbO

The lead ions have also an affinity pronounced towards $[TeO_3]$ structural units yielding the deformation of the Te–O–Te linkages. The increase of Pb^{2+} content leads to the increase of electrostatic field of the Pb^{2+} ions and consequently causes the disappearance of the $Te_2V_2O_9$ crystalline phase and pursuant to the intercalation of $[PbO_n]$ entities in the $[TeO_4]$ chain network. Then, it behaves as a glass-former for itself. The shifting of the band centered at about 950–970 cm^{-1} and the formation of the small peak at 875 cm^{-1} suggests that these changes can be explained only if we admit that the coordination number of vanadium decrease. Accordingly, the metavanadate structure is gradually changed in the pyrovanadate structure.

A mechanism high possible can be summarized as follows:

$$\begin{gathered}
2\left[TeO_{2/2}O\right]^{0} + O^{2-} \rightarrow 2\left[TeO_{3/2}O\right]^{-1} \\
Pb^{2+} + 2\left[TeO_{3/2}O\right]^{-1} \rightarrow 2\left[TeO_{2/2}O\right]^{0} + PbO \\
2TeO_2 \rightarrow 2\left[TeO_{2/2}O\right]^{0} \\
Te_2V_2O_9 \rightarrow 2TeO_2 + V_2O_5 \quad V_2O_5 \rightarrow 2\left[VOO_{3/2}\right]^{0} \\
PbO + 2\left[TeO_{2/2}O\right]^{0} \rightarrow 2\left[TeO_{3/2}O\right]^{-1} + Pb^{2+} \\
Pb^{2+} + 2\left[VO_{4/2}O\right]^{-1} \rightarrow PbO + 2\left[VOO_{3/2}\right]^{0} \\
2PbO + 4\left[VOO_{3/2}\right]^{0} \rightarrow 2\left[V_2O_{7/2}\right]^{+1} + 2\left[PbOO_{3/2}\right]^{-1}
\end{gathered}$$

However, in the glass compositions containing 50 and 60 mol%V_2O_5 the band situated at about 1020 cm^{-1} gradual vanishes and new bands centered at about ~950 cm^{-1} and 520 cm^{-1} appear. According to the mechanism suggested earlier [35, 41], the Pb^{2+} ions occupy a position between V–O–V layers. This is why they have a direct influence on the isolated V=O bonds of the [VO_5] structural units according to the scheme Pb^{2+}–O=V^{5+}. The interaction of the oxygen atom of vanadyl structural units is included in the coordination polyhedron of the lead ions leading to an elongation of the affected V=O bonds and a drop towards lower wavenumber. Such V_2O_5-rich amorphous phase can contain $Pb_xV_2O_5$ crystalline phase [38–42] in samples of glass ceramics with $x = 10$–60 mol%. In conclusion, we report a microstructural change of the amorphous V_2O_5 phase with intercalation of lead ions [40].

(v) $x = 60$ mol%PbO

Two halos characteristic of the amorphous compounds can be observed in XRD diffraction pattern. These changes can be explained only if we admit that the adding of lead oxide now participate in the network as [PbO_4] structural units yielding a change from the continuous vanadate–tellurate network to the continuous lead–vanadate–tellurate network with interconnected through Pb–O–V and Pb–O–Te bridges. The sample is formed from [PbO_4], [TeO_4], and [VO_4] structural units.

$$\begin{gathered}
2\left[V_2O_{7/2}\right]^{+1} + O^{2-} \rightarrow 2\left[V_2OO_{6/2}\right]^{0} \\
Pb^{2+} + 2\left[TeO_{3/2}O\right]^{-1} \rightarrow 2\left[TeO_{2/2}O\right]^{0} + PbO \\
V_4O_{10} \rightarrow 2\left[VO_{4/2}O\right]^{-1} + 2\left[VOO_{2/2}\right]^{+} \\
PbO + 2\left[TeO_{2/2}O\right]^{0} \rightarrow Pb^{2+} + 2\left[TeO_{3/2}O\right]^{-1} \\
Pb^{2+} + 2\left[VO_{4/2}O\right]^{-1} \rightarrow PbO + 2\left[VO_{3/2}O\right]^{0}
\end{gathered}$$

(vi) $x = 70$ mol%PbO

Further decrease in the V_2O_5 content leads to the shift of the band centered at about 990–940 cm^{-1} and the presence of new bands situated at about 760 and 870 cm^{-1}. The latter bands are usually assigned to the stretching vibrations of the orthovanadate units. The shift of the bands located from ~663 to ~698 cm^{-1} shows the conversion of [PbO_4] in [PbO_3] structural units, respectively [27, 43–51].

$$\begin{gathered}
2\left[VOO_{2/2}\right]^{+} + O^{2-} \rightarrow 2\left[VOO_{3/2}\right]^{0} \\
Pb^{2+} + 2\left[PbOO_{3/2}\right]^{-1} \rightarrow PbO + 2\left[PbOO_{2/2}\right]^{0} \\
PbO + V_4O_{10} \rightarrow Pb^{2+} + 2\left[VOO_{4/2}\right]^{-1} + 2\left[VOO_{3/2}\right]^{0} \\
PbO + 2\left[TeOO_{2/2}\right]^{0} \rightarrow Pb^{2+} + 2\left[TeOO_{3/2}\right]^{-1} \\
3Pb^{2+} + 2\left[V_2OO_{6/2}\right]^{0} \rightarrow Pb_3(VO_4)_2
\end{gathered}$$

These typical modifications of the network are illustrated in our FTIR and X-ray results by the formation of the $Pb_3(VO_4)_2$ crystalline phase and the higher intensity of characteristic band located at about 698 cm^{-1}.

(vii) $x = 80$ mol%PbO

A new peak located at about 875 cm^{-1} appears in glass ceramic. This proves that vanadium cations are incorporated in the structure of the glass ceramics as [VO_5] structural units.

$$\begin{gathered}
2\left[VOO_{3/2}\right]^{0} + O^{2-} \rightarrow 2\left[VO_{4/2}O\right]^{-1} \\
Pb^{2+} + 2\left[TeOO_{3/2}\right]^{-1} \rightarrow 2\left[TeOO_{2/2}\right]^{0} + PbO
\end{gathered}$$

(viii) $x = 90$ mol%PbO

The bands centered at about 576, 700, 768, 820, and 840 cm^{-1} are attributed to vibrations of the pyrovanadate structural units. The band located at 875 cm^{-1} shows that the vanadium exists in this compound as V^{5+} ions, in agreement with XRD pattern.

$$\begin{gathered}
2\left[VOO_{3/2}\right]^{0} + O^{2-} \rightarrow 2\left[VO_{4/2}O\right]^{-1} \\
Pb^{2+} + 2\left[VO_{4/2}O\right]^{-1} + Pb_3(VO_4)_2 \rightarrow 2Pb_2V_2O_7 \\
PbO + 2\left[TeOO_{2/2}\right]^{0} \rightarrow Pb^{2+} + 2\left[TeOO_{3/2}\right]^{-1}
\end{gathered}$$

(ix) $x = 100$ mol%PbO

The scheme of structural modifications explained above is consistent with the following:

$$\begin{gathered}
2\left[PbOO_{2/2}\right]^{0} + O^{2-} \rightarrow 2\left[PbOO_{3/2}\right]^{-1} \\
2\left[PbOO_{3/2}\right]^{-1} + Pb^{2+} \rightarrow 2\left[PbOO_{2/2}\right]^{0} + PbO
\end{gathered}$$

However, it is important to notice that the significantly different shape of the FTIR and X-ray data for this sample reveal a structural change which occurs the apparition of the PbO crystalline phase, in agreement with our mechanism.

According to these results, it can be concluded that the most lead ions are incorporated into the glass ceramic not inside clusters. The Pb^{2+} ions content is distributed into two sites attributed to the network modifier and network former.

From the FTIR investigations on structural properties of the lead–vanadate–tellurate glass ceramic system can be concluded that

(i) The increase of PbO content up to 40 mol% indicates that the lead ions have more preference for tellurate network yielding the gradual disappearance of the $Te_2V_2O_9$ crystalline phase and the conversion of $[TeO_3]$ to $[TeO_4]$ structural units.

(ii) Further addition of 50 and 60 mol%PbO produces non-bridging oxygens in the tellurate as well as in the vanadate network along with the formation of $[VO_4]$ structural units. The presence of the tetrahedrons of tellurium and vanadium facilitate the formation of amorphous phase. It is possible that longer heat-treatment time to produce lead–tellurium oxide crystalline phase.

(iii) In presence of the additional increment of PbO proportion over 60 mol% occurs considerable structural transformations, namely as breaking of the V–O–V chains, the formation of non-bridging oxygens, increase in the symmetry of V–O polyhedron, equalization of the lengths of V–O bonds, and decrease in the coordination number of vanadium. Pursuant to, the structure of these glass ceramics, investigated by means FTIR spectroscopy and X-ray diffraction studies show the presence of $Pb_3(VO_4)_2$ and $Pb_2V_2O_7$ crystalline phases.

Among these unconventional vanadate–tellurate glasses and glass ceramics, network formers are good host material for lead ions, capable to intercalate a variety of neutral and changed species such as $Te_2V_2{}^{5+}O_9$, $Pb_3(V^{5+}O_4)_2$, $Pb_2V_2{}^{5+}O_7$ and V_2O_5-rich amorphous phase.

The V_2O_5-rich amorphous phase usually retains a lamellar structure with the guest species of lead ions occupying the interlayer region. Such layered transition metal oxides can be attracted a considerable attention due to their applications in ion exchange, catalysis, semiconductor, and active cathode materials.

In brief, these glass ceramics contain V^{4+} and V^{5+} ions necessary for the electrical conduction. It is of great interest to point out that the intensities of two broad peaks at $\sim$520 and 650 cm^{-1}, due to the stretching modes of V–O-V single bonds, decreases significantly with lead ions insertion. When lead ions and electrons are inserted into lead–vanadate–tellurate glass ceramics, the electrons reduce V^{5+} ions to V^{4+}, thus creating V^{4+}=O bonds. Because these new double bonds are weaker than the typical double bonds involving V^{5+} ions, their corresponding IR peak appears at lower energy than that for the V^{5+}=O bonds. Also all glass ceramics show the peak centered at about $\sim$950 cm^{-1}, we conclude that there are some V^{4+} ions in as-deposited glass ceramics as well.

Based on these experimental results, we propose that the V^{4+}=O bonds are created by two different mechanisms:

(i) As already mentioned, one is the direct conversion of V^{5+}=O bonds to V^{4+}=O bonds with lead ions insertion. When V^{5+}–O–V^{5+} single bonds are reduced to the V^{4+}–O–V^{4+} bonds with lead insertion, the distances between V and O become longer due to the weaker coulomb interaction and these bonds can be broken, thus creating the V^{4+}=O bonds. For samples with $10 \leq x \leq 60$ mol% PbO, variations observed in the FTIR spectra and X-ray diffraction patterns, namely the gradual disappearance of the $Te_2V_2{}^{5+}O_9$ crystalline phase and V_2O_5-rich amorphous phase, are consistent with the scheme of modification explained above.

These evolutions of the structures of glass ceramics can be explained considering that the lead ions are firstly inserted in the divalent state and they can be considered as modifiers because they have a strong affinity towards these groups containing non-bridging oxygens, which are negative-charged (as TeO_n structural units). On the other hand, the Pb^{2+} ions occupy a position between the V–O–V layers. This is why they have a direct influence on the isolated V=O bonds of the $[VO_5]$ units the scheme Pb^{2+}–O=V^{5+}. Under that interaction, the atom of the vanadyl units is included in the Pb coordination polyhedron and the lead ions yield an elongation of the affected V=O bonds and a drop in wavenumber down to 950 cm^{-1}.

(ii) The other is the breaking of V^{4+}–O–V^{4+} single bonds ($x > 60$ mol%PbO). We believe that this second process of transformation of V^{4+}–O–V^{4+} bonds at the V^{5+}–O–V^{5+} bonds generates a more disordered structure with lead oxide insertion. These typical modifications of the network are illustrated in our FTIR and X-ray results by the formation of the $Pb_3(V^{5+}O_4)_2$ and $Pb_2V_2{}^{5+}O_7$ crystalline phases.

These evolutions of the structures of glass ceramics can be explained considering the accommodation of the network with excess of oxygen by the formation of $[PbO_n]$ structural units and pursuant to the intercalation of $[PbO_n]$ entities in the $[TeO_n]$ and $[VO_n]$ chain network.

Conclusions

We have examined and analyzed the effects of systematic intercalation of the lead ions in the host matrix with interesting results using the FTIR spectroscopy and X-ray diffraction investigations.

The FTIR spectra of the unconventional glass ceramics show some bands around 520 and 650 cm^{-1}, due to the stretching mode of the V–O–V bonds, a relatively sharp band at $\sim$1020 cm^{-1} due to the V^{5+}=O stretching mode of terminal oxygen atoms and a band at $\sim$950 cm^{-1} that moves towards lower wavenumbers by increasing of lead ions content. This latter band shows vibrations of V^{4+}=O bonds.

Based on FTIR and XRD results, we found that the V^{4+}=O bonds are generated by two different mechanisms. One is the direct conversion of V^{5+}=O bonds to V^{4+}=O bonds with insertion of lead ions. The other mechanism is due to the breaking of V^{4+}–O–V^{4+} single bonds.

References

1. Harishima H, Ide M, Yoshida T (1986) J Non-Cryst Solids 86:327
2. Ovshinsky SR (1968) Phys Rev Lett 21:1450
3. Montani RA, Levy M, Souquet JL (1992) J Non-Cryst Solids 149:249
4. Ghosh A (1988) J Appl Phys 64:2652
5. Shaju KM, Chandra S (1995) J Mater Sci 30:3457. doi:10.1007/BF00349894
6. Turky G, Dawy M (2002) Mater Chem Phys 77:48
7. Mayer H, Pupp G (1977) Z Kristallogr 145:321
8. Frechero MA, Quinzani OV, Pettigrosso RS, Villar M, Montani RA (2007) J Non-Cryst Solids 353:2919
9. Charton P, Gengembre L, Armand P (2002) J Solid State Chem 168:175
10. Rada S, Culea M, Rada M, Culea E (2008) J Mater Sci 43(18):6122. doi:10.1007/s10853-008-2939-9
11. Rada S, Culea E, Rus V, Pica M, Culea M (2008) J Mater Sci 43:3713. doi:10.1007/s10853-008-2601-6
12. Manara D, Grandjean A, Pinet O, Dussossoy JL, Neuville DR (2007) J Non-Cryst Solid 353:12
13. Iordanova R, Dimitrov V, Klissurski D (1994) J Non-Cryst Solids 58:58
14. Mandal S, Ghosh A (1994) Phys Rev B 49:3131
15. Sen S, Ghosh A (1999) J Phys Condens Matter 11:1529
16. Ghosh A (1995) J Chem Phys 102:1385
17. Rada S, Culea E, Rada M, Pascuta P, Maties V (2009) J Mater Sci 44:3235. doi:10.1007/s10853-009-3433-8
18. Sidkey MA, El Mallawany R, Sidkey MA, Nakhla RI, Abd El-Moneim A (1997) J Non-Cryst Solid 215:75
19. Rada S, Culea M, Neumann M, Culea E (2008) Chem Phys Lett 460:196
20. Rada S, Pascuta P, Culea M, Maties V, Rada M, Barlea M, Culea E (2009) J Mol Struct 924–926:89
21. Ghosh A (1990) Phys Rev B 42:5665
22. Ghosh A (1989) J Appl Phys 66:2425
23. Ghosh A, Chakravorty D (1993) Phys Rev B 48:5167
24. Ghosh A, Pan A (2000) Phys Rev Lett 84:2188
25. Pan A, Ghosh A (1999) Phys Rev B 60:3224
26. Pan A, Ghosh A (1999) Phys Rev B 59:899
27. Mandal S, Ghosh A (1993) Phys Rev B 48:9388
28. Darriet J, Galy J (1973) Cryst Struct Commun 2:237
29. Sudarsan V, Kulshreshtha SK (1999) J Non-Cryst Solids 258:20
30. Rada S, Culea E, Culea M (2008) J Mater Sci 43(19):6480. doi:10.1007/s10853-008-2980-8
31. Denton EP, Rawson H, Stanworth JE (1954) Nature 173:1030
32. Sen S, Ghosh A (2001) J Phys Condens Matter 13:1979
33. Sen S, Ghosh A (2000) J Mater Res 15:995
34. Sen S, Ghosh A (1999) J Non-Cryst Solids 258:29
35. Shivachev BL, Petrov T, Yoneda H, Titorenkova R, Mihailova B (2009) Scripta Mater 61(5):493
36. Ghosh A (1990) Philos Mag B 61:87
37. Dimitrov V, Dimitrov Y (1990) J Non-Cryst Solids 122:133
38. Fares V, Magini M, Montenero A (1988) J Non-Cryst Solids 99:1353
39. Dimitrov V (1995) J Non-Cryst Solids 192:183
40. Dimitrov V (1987) J Solid State Chem 66:256
41. Hayakawa S, Yoko T, Sakka S (1994) J Ceram Soc Jpn 102:530
42. Fredrickson LD, Hausen DM (1963) Anal Chem 35:825
43. Rivoalen L, Revcolevschi A, Livage J, Collongues R (1976) J Non-Cryst Solids 21:171
44. Rada S, Culea M, Culea E (2008) J Phys Chem A 112(44):11251
45. Rada S, Culea E (2009) J Mol Struct 929(1–3):141
46. Mandal S, Hazra S, Das D, Ghosh A (1995) J Non-Cryst Solids 183:315
47. Ramesh KV, Sastry DL (2006) J Non-Cryst Solids 352:5421
48. Mandal S, Hazra S, Ghosh A (1994) J Mater Sci Lett 13:1054
49. Hazra S, Ghosh A (1995) J Mater Res 10:2374
50. Milanova M, Iardanova R, Kostov KL (2009) J Non-Cryst Solids 355:379
51. Rada S, Ristoiu T, Rada M, Coroiu I, Maties V, Culea E (2010) Mater Res Bull 45:69